



Article scientifique

Article

2020

Accepted version

Open Access

This is an author manuscript post-peer-reviewing (accepted version) of the original publication. The layout of the published version may differ .

---

## Fluorescent Membrane Tension Probes for Super-Resolution Microscopy: Combining Mechanosensitive Cascade Switching with Dynamic-Covalent Ketone Chemistry

---

Garcia, José; Maillard, Jimmy Stéphane; Furera, Ina; Strakova, Karolina; Colom Diego, Adai;  
Mercier, Vincent; Roux, Aurélien; Vauthey, Eric; Sakai, Naomi; Fuerstenberg, Alexandre; Matile, Stefan

### How to cite

GARCIA, José et al. Fluorescent Membrane Tension Probes for Super-Resolution Microscopy: Combining Mechanosensitive Cascade Switching with Dynamic-Covalent Ketone Chemistry. In: Journal of the American Chemical Society, 2020, vol. 142, n° 28, p. 12034–12038. doi: 10.1021/jacs.0c04942

This publication URL: <https://archive-ouverte.unige.ch//unige:138589>

Publication DOI: [10.1021/jacs.0c04942](https://doi.org/10.1021/jacs.0c04942)

## Fluorescent Membrane Tension Probes for Super-Resolution Microscopy: Combining Mechano-sensitive Cascade Switching with Dynamic-Covalent Ketone Chemistry

José García-Calvo, Jimmy Maillard, Ina Fureraj, Karolina Strakova, Adai Colom, Vincent Mercier, Aurelien Roux, Eric Vauthey, Naomi Sakai, Alexandre Fürstenberg\* and Stefan Matile\*

School of Chemistry and Biochemistry, University of Geneva, Geneva, Switzerland

**ABSTRACT.** We report design, synthesis, and evaluation of fluorescent flipper probes for single-molecule super-resolution imaging of membrane tension in living cells. Reversible switching from bright-state ketones to dark-state hydrates, hemiacetals, and hemithioacetals is demonstrated for twisted and planarized mechanophores in solution and membranes. Broadband femtosecond fluorescence up-conversion spectroscopy evinces ultrafast chalcogen-bonding cascade switching in the excited state in solution. According to fluorescence lifetime imaging microscopy, the new flippers image membrane tension in live cells with record red shifts and photostability. Single-molecule localization microscopy with the new tension probes resolves membranes well below the diffraction limit.

The imaging of physical forces in living systems is a central challenge in current biology.<sup>1</sup> To contribute solutions, we have introduced small-molecule chemistry tools to image membrane tension in living cells.<sup>2</sup> Based on the concept of planarizable push-pull probes,<sup>3,4</sup> the so-called flipper probes allowed us to image the change of plasma<sup>5</sup> and organellar membrane tension in living cells.<sup>6</sup> Flipper probes are twisted dithiophene (DTT) push-pull dimers (Figure 1a). Their mechanical planarization in the ground state

couples the push-pull system and shifts the absorption to the red. Chalcogen-bonding cascade switching (CS) has been added because donors and acceptors are needed for red shifts in planar but incompatible with twisted conformers.<sup>7</sup> With CS, triazole donors and aldehyde acceptors turn-on only once planarization inverts the depth of the  $\sigma$  holes and thus the respective chalcogen bonds (Figure 1a, dashed).

The aldehyde acceptor in CS flipper **1** attracted our attention because it promised access to super-resolution (SR) imaging. Single-molecule based SR microscopy requires fluorophores to switch between bright and dark states.<sup>8–10</sup> This on-off switching has been realized in several elegant ways, such as partitioning, oligomerizations, photoswitches and reversible conjugate additions.<sup>9,11,12</sup> Less explored in SR imaging, dynamic-covalent 1,2-addition to carbonyls is receiving current attention in the context of dynamic libraries, enzyme inhibitors, sensors and materials covering hydrates, hemiacetals, hemithioacetals, and hemiaminals.<sup>13,14</sup> In the following, we report design, synthesis, and evaluation of the first SR flipper probe for single-molecule localization microscopy (SMLM).

With a more electrophilic version of the aldehyde in flipper **1**, we expected that nucleophilic addition to ketone acceptors could occur spontaneously, destroy the push-pull system and thus afford the reversible dark state needed for photoswitching. We selected a trifluoromethyl ketone<sup>14</sup> as acceptor in **2** ( $\sigma_p = 0.80$ ,<sup>15</sup> Figure 1b), alkyl ketones **3** and **4** as controls.

Amphiphiles **2–4** and their hydrophobic analogs **5–6** were prepared by multistep organic synthesis (Figures 1b,c, Schemes S1-S3).<sup>2</sup> The ketones were introduced in the early stage of synthesis. Weinreb synthesis with DTT **7** and amides **8** gave ketones **9**. Oxidation and bromination afforded intermediates **10**, which were transformed into **2-6** following established routes.

In solution, hydration of the twisted ketone **5T** was visible to the naked eyes (Figure 1a,d). In the absorption spectrum, this change corresponded to a blue shift from 450 to 400 nm (Figure 1e). In the excitation spectrum, the 450 nm band disappeared but the 400 nm band did not appear (Figure 1f). This difference originates from the lower quantum yield of **5Td** (4%) compared to **5T** (27%, Figure S8). Hill analysis of both spectra gave an  $EC_{50} = 130$  mM, describing the effective water concentration needed for

50% hydration (Figure 1g■). Dark-state (hemi)acetals and hemithioacetals formed with MeOH, ethylene glycol and octanethiol. As a diol, ethyleneglycol had an  $EC_{50} = 0.7$  M half the  $EC_{50} = 1.3$  M of MeOH (Figure 1g●→▲). Conversion of octanethiol into the more nucleophilic octanethiolate lowered the  $EC_{50}$  to 130 mM (◆→■). Only the bulky t-BuOH failed to add to **5T** (▼).

The 1,2-addition occurred in wet polar solvents with **5** but not with **6** (Figure 1h,i). As a result, **6** showed positive solvatochromism with the  $\Delta\mu \sim 13$  D known for twisted flippers (Figures 1i,S2-S4).<sup>4,16</sup> In contrast, trends for **5** were disturbed by dynamic covalent ketone chemistry (Figure 1h). The large Stokes shifts are observed in solution because twisted flippers **T** absorb but planar flippers **P\*** emit.<sup>16</sup> Their emission wavelength is mechano-insensitive for this reason. Different from most other membrane probes that sense off-equilibrium in the excited state,<sup>11,17,18</sup> flippers thus respond in the ground state to physical forces applied through confining surroundings.<sup>7</sup>

Broadband femtosecond fluorescence up-conversion spectroscopy (FLUPS)<sup>19,20</sup> revealed the time evolution of the fluorescence spectrum of **6T** in DMSO after 400 nm excitation. Directly after excitation, the emission maximized around 560 nm and then rapidly shifted outside the experimental spectral window (Figure 1j). The biexponential Stokes shift dynamics of

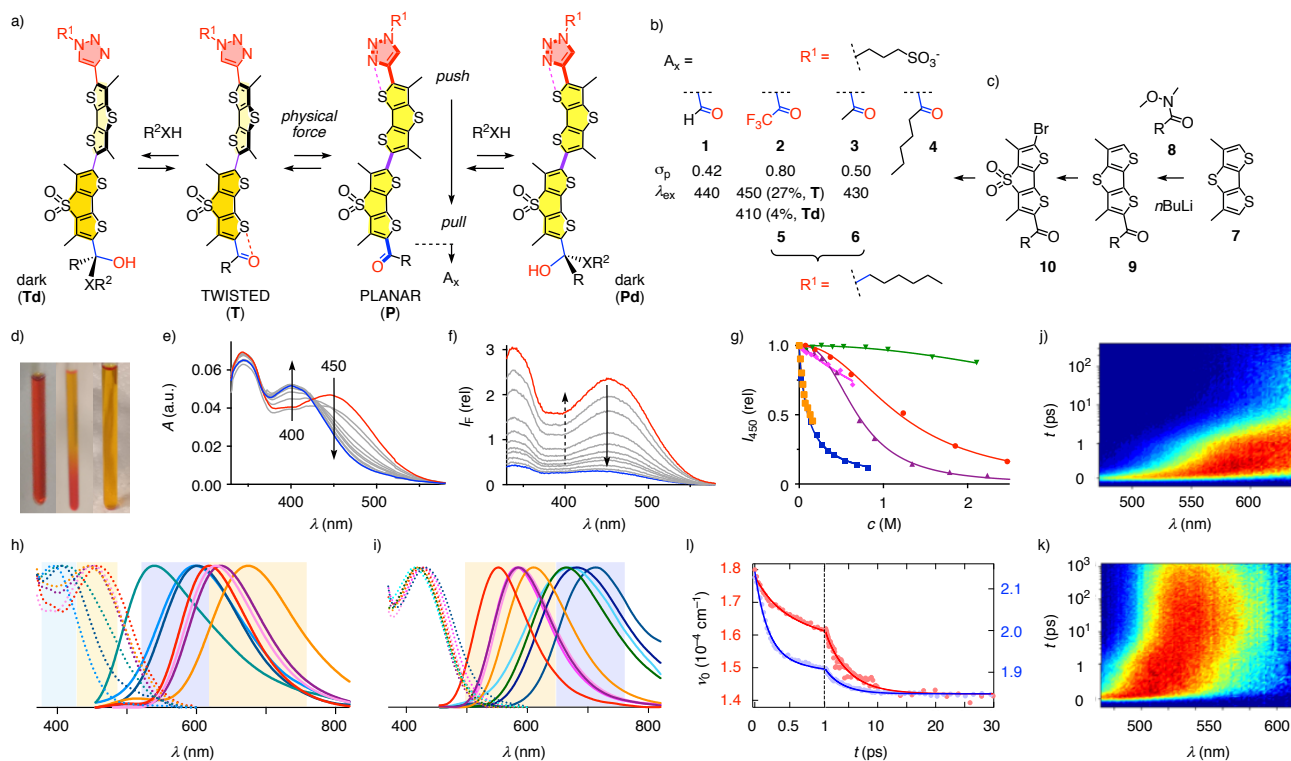


**Figure 1.** a) Design, b) structure, c) synthesis and d-l) solution studies of SR-CS flippers. a) Dynamic-covalent addition to ketones to turn off (d) twisted (T) and planar (P) mechanophores containing chalcogen-bonding (dashed) CS to turn on donors and acceptors ( $A_x$ ) in P only. b) Flippers 1-6 with Hammett  $\sigma_p$ , excitation maxima (in nm) and fluorescence quantum yields (dioxane). c) Introduction of ketones during flipper synthesis. d) Addition of a drop of  $D_2O$  to **5** in  $THF-d_8$  in an NMR tube (left to right). e) Absorption and f) excitation spectra ( $\lambda_{em}$  600 nm) of **5** (2  $\mu M$ ) in dioxane with increasing concentration of water (red to blue, 0 – 820 mM, g, blue■). g) Fluorescence excitation intensity at 450 nm of **5** (2  $\mu M$ ) in dioxane with increasing concentrations of water (blue■), MeOH (red●), octanethiolate (octanethiol in dioxane with 0.25% triethylamine; orange■) and octanethiol (magenta◆), ethyleneglycol (purple▲) and tBuOH (green▼). h) Absorption (dashed), and emission spectra (solid,  $\lambda_{ex}$  435 nm) of **5** (1  $\mu M$ ) in less (orange, T) and more polar solvents (blue, Td); i) same for **6** (all T; details: Figures S2-S4). j) Time-resolved emission spectra of **6** in DMSO after femtosecond excitation at 400 nm ( $I$  from blue (0) to red); k) same for coumarin 153. l) Time dependence of emission maximum of **6** (red) and coumarin 153 (blue) with multiexponential fit (from j, k).

**6T** was much slower than that of coumarin C153<sup>21</sup> (Figure 1k,l). As solvent relaxation dynamics are independent of the probe,<sup>19,22</sup> this difference demonstrated that flippers undergo significant structural relaxation upon excitation, namely planarization to **6P\***. During this process, the donor and acceptor subunits are turned on, leading to a significant increase of the electric dipole moment (Figure 1a) and thus to red-shifting solvent relaxation.

Flipper **2** partitioned without much preference into the liquid-disordered ( $L_d$ ) membranes of 1,2-dioleoyl 3-*sn*-phosphatidylcholine (DOPC) and liquid-ordered ( $L_o$ ) membranes of sphingomyelin/cholesterol (SM/CL) large-unilamellar vesicles (LUVs, Figures 2a,e,S29). The excitation maximum in  $L_o$  membranes showed characteristic finestructure with the 0-0 transition at 560 and the 0-1 at 526 nm, and the third band at 492 nm (Figure 2b,d). This emergence of vibrational finestructure is consistent with reduced flipper dynamics in  $L_o$  environments.<sup>16</sup>

The excitation peak of **2** was red shifted (560 nm) and strong in  $L_o$ , but blue shifted (418 nm) and weak in  $L_d$  membranes (Figure 2b,e). Both red shift and intensity increase upon changing from  $L_d$  to  $L_o$  membranes were more significant than with **1**, **3** and **4** (Figures 2b,c,e). The transition from twisted hydrate **2Td** in  $L_d$  to planar ketone **2P** in  $L_o$  membranes is likely to account for such an excellent performance. This conclusion was consistent with both the better hydration of  $L_d$  membranes<sup>17,23</sup> and less electrophilic ketones in **2P** compared to **2T**.

To image membrane tension, the increase in fluorescence lifetime with red-shifting flipper planarization provides access to fluorescence lifetime imaging microscopy (FLIM). In biologically relevant membranes, lifetimes increase with tension because of membrane reorganization (Figure 3a).<sup>6</sup> Compared to **1**, FLIM of **2** in giant unilamellar vesicles (GUVs) gave longer lifetimes in  $L_o$  and shorter ones in  $L_d$  membranes, that is increased mechanosensitivity (Figures 3c,d,2a).

Confocal laser scanning microscopy (CLSM) images of **2** added to HeLa cells showed brightly emitting plasma membranes, clearly brighter than **1**, **3** and **4** (Figure 3b). FLIM images of **2** in HeLa cells gave

$\tau_{\text{iso}} = 4.1$  ns before and  $\tau_{\text{hyper}} = 3.7$  ns after osmotic shock (Figure 3e,f). This mechanosensitivity was similar to **1** (3.7→3.4 ns) and Flipper-TR<sup>®</sup> (4.8→4.2 ns), considering that absolute values can vary also because of unrelated factors such as cell density. Unlike Flipper-TR<sup>®</sup>,<sup>5</sup> **2** also entered into the endocytic cycle. The lower  $\tau_{\text{iso}}$  in early endosomes was as expected for their more fluid membranes.<sup>6</sup> Isolate FLIM analysis of **2** in endosomes matched with 3.7→3.3 ns exactly the mechanosensitivity of Flipper-TR<sup>®</sup> targeted to endosomes and lysosomes.<sup>6</sup> Most importantly, **2** bleached slower than Flipper-TR<sup>®</sup> (Figure 3g). This difference presumably originated from the increased chemical stability secured with cascade switching.<sup>8</sup>

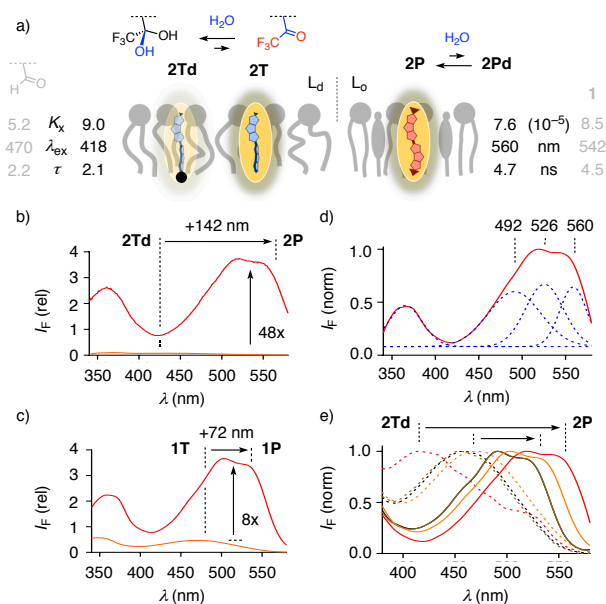


**Figure 2.** a) SR flipper **2** in  $L_d$  (DOPC) and  $L_o$  (SM/CL) LUVs with partition coefficients  $K_x$ , excitation maxima, and fluorescence lifetimes (from GUVs), compared to **1** (grey). b) Excitation spectra ( $\lambda_{\text{em}} 600$  nm) of **2** (100 nM) in DOPC (orange) and SM/CL (7:3) (red) LUVs (75  $\mu\text{M}$  lipid, 10 mM Tris, 100 mM NaCl, pH 7.4); c) same for **1**. d) Deconvoluted excitation spectrum of **2** in SM/CL (7:3) LUVs. e) Normalized excitation spectra of **3** ~ **4** (black), **1** (orange) and **2** (red) in SM/CL (7:3) (solid) compared to DOPC LUVs (dashed).

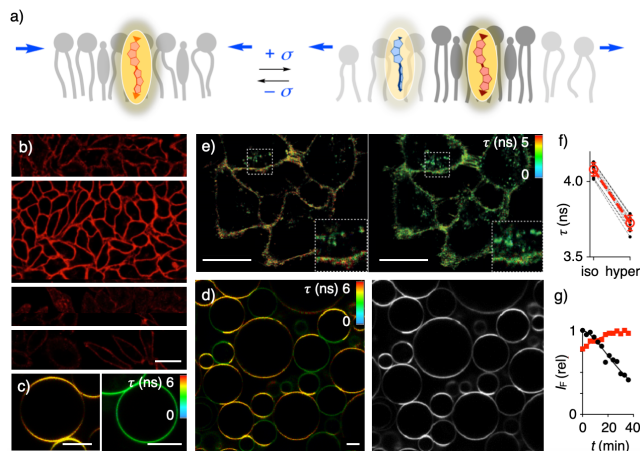


**Figure 3.** a) Flipper probes reporting membrane tension in mixed membranes as an increase in lifetime. b) CSLM images of **1–4** (2  $\mu\text{M}$ , top down, **2** enlarged) in HeLa Kyoto cells. c) FLIM images of **2** in SM/CL (7:3) (yellow: 4.7 ns) and DOPC GUVs (green: 2.1 ns), d) FLIM (left) and fluorescence intensity images (right) of **2** (1  $\mu\text{M}$ ) in L<sub>o</sub>/L<sub>d</sub> SM/CL/DOPC (4:3:3) GUVs, e) FLIM images of **2** (1  $\mu\text{M}$ ) in HeLa MZ cells before (left) and after hyperosmotic shock (right, inset: magnified endosomes). f) Lifetime measurements from 2 independent experiments as shown in (e). Thick line: mean  $\pm$  SD of the 11 fields from 2 experiments (thin lines, two-tailed paired *t*-test:  $P < 0.0001$ ). g) Fluorescence intensity of **2** (red) and Flipper-TR<sup>®</sup> (black, 1  $\mu\text{M}$ ) in HeLa cells with time. Scale bars: b) 40  $\mu\text{m}$ ; c, d) 10  $\mu\text{m}$ ; e) 20  $\mu\text{m}$ .

Super-resolution imaging with flipper **2** in L<sub>o</sub> lipid environments was explored by SMLM using the point accumulation for imaging in nanoscale topography (PAINT) method.<sup>24</sup> Addition of **2** to L<sub>o</sub> GUVs deposited on a glass coverslip led to the observation of single fluorescent molecules stochastically lighting up in the membrane of the GUV (Figure 4a). The stochastic nature of the emission can be explained by individual molecules of flipper **2** in the solution pool partitioning to the membrane and becoming emissive before diffusing out again or photobleaching. However, the inactivity of Flipper-TR<sup>®</sup> in similar experiments supported that the dynamic covalent ketone chemistry unique for flipper **2** might contribute to its stochastic emission. Excitation at 515 nm ensured good selectivity for the **2P** form. Subsequent localization of several thousands of these single emitters enabled the reconstruction of a super-resolution image of the GUV membrane in the focal plane (Figure 4c). Cross-sections of the membrane display full widths

at half maximum (FWHM) as low as  $\sim 40$  nm (Figure 4d), which is well below the diffraction limit and the measured FWHM of 220 nm in the diffraction-limited image of the same GUV (Figure 4b). With an average of  $\sim 1500 \pm 700$  photons detected per localization (Figure 4e), the predicted mean localization precision<sup>25</sup> was about  $15 \pm 10$  nm in this experiment (Figure 4f), values comparable to classical PAINT probes.<sup>26</sup>

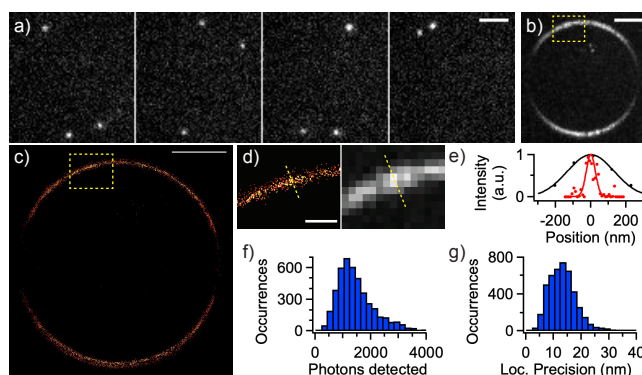


**Figure 4.** PAINT-SMLM images of SM/CL (7:3) GUVs with **2** (6 nM). a) Stochastic emission of single molecules of **2** in the L<sub>o</sub> membrane of a GUV. b) Diffraction-limited and c) PAINT super-resolution image of the same GUV as in a). d) Magnified view of regions in boxes in b) and c). e) Cross-sections of the GUV membrane indicated by a line in d) display a profile width well-below the diffraction limit (FWHM of  $42 \pm 5$  nm vs.  $220 \pm 8$  nm in the diffraction-limited image). f) Distribution of photons detected per frame from single molecules of **2** in the GUV shown in c). g) Distribution of localization precision computed from the photon distribution in f). Scale bars: a), b), c): 2  $\mu$ m; d): 500 nm.

Although chalcogen-bonding cascade switching of planarizable push-pull probes might seem already conceptually demanding, this study adds another layer of complexity with dynamic covalent carbonyl chemistry. The results of this cumulation of supramolecular concepts are record performances throughout (e.g., red shifts, photostability), access to blinking mechanophores and, most importantly, super-resolution imaging. These results open great perspectives, from probe design to imminent use in biology.

## ASSOCIATED CONTENT

### Supporting Information

Detailed experimental procedures. This material is available free of charge at <http://pubs.acs.org>.

## AUTHOR INFORMATION

### Corresponding Author

\*[stefan.matile@unige.ch](mailto:stefan.matile@unige.ch), [alexandre.fuerstenberg@unige.ch](mailto:alexandre.fuerstenberg@unige.ch)

### Notes

The authors declare the following competing financial interest: The University of Geneva has licensed Flipper-TR<sup>®</sup> to Spirochrome for commercialization.

## ACKNOWLEDGMENT

We thank NMR, MS and Bioimaging platforms for services, and the University of Geneva, the NCCR Chemical Biology, the NCCR Molecular Systems Engineering and the Swiss NSF for financial support.

## REFERENCES

- (1) (a) Pontes, B.; Monzo, P.; Gauthier, N. C. Membrane Tension: A Challenging but Universal Physical Parameter in Cell Biology. *Semin. Cell Dev. Biol.* **2017**, *71*, 30–41. (b) Diz-Muñoz, A.; Weiner, O. D.; Fletcher, D. A. In Pursuit of the Mechanics That Shape Cell Surfaces. *Nat. Phys.* **2018**, *14*, 648–652.
- (2) Strakova, K.; Assies, L.; Goujon, A.; Piazzolla, F.; Humeniuk, H. V.; Matile, S. Dithienothiophenes at Work: Access to Mechanosensitive Fluorescent Probes, Chalcogen-Bonding Catalysis, and Beyond. *Chem. Rev.* **2019**, *119*, 10977–11005.
- (3) Fin, A.; Vargas Jentzsch, A.; Sakai, N.; Matile, S. Oligothiophene Amphiphiles as Planarizable and Polarizable Fluorescent Membrane Probes. *Angew. Chem. Int. Ed.* **2012**, *51*, 12736–12739.

- (4) Dal Molin, M.; Verolet, Q.; Colom, A.; Letrun, R.; Derivery, E.; Gonzalez-Gaitan, M.; Vauthey, E.; Roux, A.; Sakai, N.; Matile, S. Fluorescent Flippers for Mechanosensitive Membrane Probes. *J. Am. Chem. Soc.* **2015**, *137*, 568–571.
- (5) Colom, A.; Derivery, E.; Soleimanpour, S.; Tomba, C.; Molin, M. D.; Sakai, N.; González-Gaitán, M.; Matile, S.; Roux, A. A Fluorescent Membrane Tension Probe. *Nat. Chem.* **2018**, *10*, 1118–1125.
- (6) Goujon, A.; Colom, A.; Straková, K.; Mercier, V.; Mahecic, D.; Manley, S.; Sakai, N.; Roux, A.; Matile, S. Mechanosensitive Fluorescent Probes to Image Membrane Tension in Mitochondria, Endoplasmic Reticulum, and Lysosomes. *J. Am. Chem. Soc.* **2019**, *141*, 3380–3384.
- (7) Macchione, M.; Goujon, A.; Strakova, K.; Humeniuk, H. V.; Licari, G.; Tajkhorshid, E.; Sakai, N.; Matile, S. A Chalcogen-Bonding Cascade Switch for Planarizable Push–Pull Probes. *Angew. Chem. Int. Ed.* **2019**, *58*, 15752–15756.
- (8) Fürstenberg, A.; Heilemann, M. Single-Molecule Localization Microscopy – near-Molecular Spatial Resolution in Light Microscopy with Photoswitchable Fluorophores. *Phys. Chem. Chem. Phys.* **2013**, *15*, 14919–14930.
- (9) Wang, L.; Frei, M. S.; Salim, A.; Johnsson, K. Small-Molecule Fluorescent Probes for Live-Cell Super-Resolution Microscopy. *J. Am. Chem. Soc.* **2019**, *141*, 2770–2781.
- (10) (a) Kuo, C.; Hochstrasser, R. M. Super-Resolution Microscopy of Lipid Bilayer Phases. *J. Am. Chem. Soc.* **2011**, *133* (13), 4664–4667. (b) Ha, T.; Tinnefeld, P. Photophysics of Fluorescent Probes for Single-Molecule Biophysics and Super-Resolution Imaging. *Annu. Rev. Phys. Chem.* **2012**, *63*, 595–617. (c) Sezgin, E. Super-Resolution Optical Microscopy for Studying Membrane Structure and Dynamics. *J. Phys. Condens. Matter* **2017**, *29*, 273001. (d) Parmryd, I.; Eggeling, C. Super-Resolution Optical Microscopy of Lipid Plasma Membrane Dynamics. *Essays Biochem.* **2015**, *57*, 69–80.
- (11) (a) Xiong, Y.; Vargas Jentsch, A.; Osterrieth, J. W. M.; Sezgin, E.; Sazanovich, I. V.; Reglinski, K.; Galiani, S.; Parker, A. W.; Eggeling, C.; Anderson, H. L. Spiroanthoxazine Switchable Dyes for Biological Imaging. *Chem. Sci.* **2018**, *9*, 3029–3040. (b) Danylchuk, D. I.; Moon, S.; Xu, K.;

Klymchenko, A. S. Switchable Solvatochromic Probes for Live-Cell Super-resolution Imaging of Plasma Membrane Organization. *Angew. Chem. Int. Ed.* **2019**, *58*, 14920–14924.

(12) (a) Dempsey, G. T.; Bates, M.; Kowtoniuk, W. E.; Liu, D. R.; Tsien, R. Y.; Zhuang, X. Photoswitching Mechanism of Cyanine Dyes. *J. Am. Chem. Soc.* **2009**, *131*, 18192–18193. (b) Wijesooriya, C. S.; Peterson, J. A.; Shrestha, P.; Gehrmann, E. J.; Winter, A. H.; Smith, E. A. A Photoactivatable BODIPY Probe for Localization-Based Super-Resolution Cellular Imaging. *Angew. Chem. Int. Ed.* **2018**, *57*, 12685–12689.

(13) (a) Drahoňovský, D.; Lehn, J.-M. Hemiacetals in Dynamic Covalent Chemistry: Formation, Exchange, Selection, and Modulation Processes. *J. Org. Chem.* **2009**, *74*, 8428–8432. (b) Caraballo, R.; Dong, H.; Ribeiro, J. P.; Jiménez-Barbero, J.; Ramström, O. Direct STD NMR Identification of  $\beta$ -Galactosidase Inhibitors from a Virtual Dynamic Hemithioacetal System. *Angew. Chem. Int. Ed.* **2010**, *49*, 589–593. (c) Sakulsombat, M.; Zhang, Y.; Ramström, O. Dynamic Asymmetric Hemithioacetal Transformation by Lipase-Catalyzed  $\gamma$ -Lactonization: In Situ Tandem Formation of 1,3-Oxathiolan-5-One Derivatives. *Chem. Eur. J.* **2012**, *18*, 6129–6132. (d) Zhang, Y.; Hu, L.; Ramström, O. Double Parallel Dynamic Resolution through Lipase-Catalyzed Asymmetric Transformation. *Chem. Commun.* **2013**, *49*, 1805–1807. (e) You, L.; Anslyn, E. V. Secondary Alcohol Hemiacetal Formation: An in Situ Carbonyl Activation Strategy. *Org. Lett.* **2009**, *11*, 5126–5129. (f) Kolesnichenko, I. V.; Anslyn, E. V. Practical Applications of Supramolecular Chemistry. *Chem. Soc. Rev.* **2017**, *46*, 2385–2390. (g) Brachvogel, R.-C.; von Delius, M. The Dynamic Covalent Chemistry of Esters, Acetals and Orthoesters. *Eur. J. Org. Chem.* **2016**, *2016*, 3662–3670. (h) Qian, Y.; Karpus, J.; Kabil, O.; Zhang, S.-Y.; Zhu, H.-L.; Banerjee, R.; Zhao, J.; He, C. Selective Fluorescent Probes for Live-Cell Monitoring of Sulphide. *Nat. Commun.* **2011**, *2*, 1506.

(14) (a) Mertz, E.; Zimmerman, S. C. Cross-Linked Dendrimer Hosts Containing Reporter Groups for Amine Guests. *J. Am. Chem. Soc.* **2003**, *125*, 3424–3425. (b) Sasaki, S.; Kotegawa, Y.; Tamiaki, H. Trifluoroacetyl-Chlorin as a New Chemosensor for Alcohol/Amine Detection. *Tetrahedron Lett.* **2006**,

47, 4849–4852. (c) Xu, Y.; Yu, S.; Wang, Y.; Hu, L.; Zhao, F.; Chen, X.; Li, Y.; Yu, X.; Pu, L. Ratiometric Fluorescence Sensors for 1,2-Diamines Based on Trifluoromethyl Ketones. *Eur. J. Org. Chem.* **2016**, *2016*, 5868–5875. (d) Mohr, G. J.; Lehmann, F.; Grummt, U.-W.; Spichiger-Keller, U. E. Fluorescent Ligands for Optical Sensing of Alcohols: Synthesis and Characterisation of p-N,N-Dialkylamino-Trifluoroacetylstilbenes. *Anal. Chim. Acta* **1997**, *344*, 215–225. (e) Mohr, G. J. New Chromoreactands for the Detection of Aldehydes, Amines and Alcohols. *Sens. Actuators B Chem.* **2003**, *90*, 31–36.

(15) Hansch, C.; Leo, A.; Taft, R. W. A Survey of Hammett Substituent Constants and Resonance and Field Parameters. *Chem. Rev.* **1991**, *91*, 165–195.

(16) Strakova, K.; Poblador-Bahamonde, A. I.; Sakai, N.; Matile, S. Fluorescent Flipper Probes: Comprehensive Twist Coverage. *Chem. Eur. J.* **2019**, *25*, 14935–14942.

(17) Klymchenko, A. S. Solvatochromic and Fluorogenic Dyes as Environment-Sensitive Probes: Design and Biological Applications. *Acc. Chem. Res.* **2017**, *50*, 366–375.

(18) (a) Ashoka, A. H.; Ashokkumar, P.; Kovtun, Y. P.; Klymchenko, A. S. Solvatochromic Near-Infrared Probe for Polarity Mapping of Biomembranes and Lipid Droplets in Cells under Stress. *J. Phys. Chem. Lett.* **2019**, *10*, 2414–2421. (b) Sherin, P. S.; López-Duarte, I.; Dent, M. R.; Kubánková, M.; Vyšniauskas, A.; Bull, J. A.; Reshetnikova, E. S.; Klymchenko, A. S.; Tsentalovich, Y. P.; Kuimova, M. K. Visualising the Membrane Viscosity of Porcine Eye Lens Cells Using Molecular Rotors. *Chem. Sci.* **2017**, *8*, 3523–3528. (c) Kulkarni, R. U.; Miller, E. W. Voltage Imaging: Pitfalls and Potential. *Biochemistry* **2017**, *56*, 5171–5177. (d) Chambers, J. E.; Kubánková, M.; Huber, R. G.; López-Duarte, I.; Avezov, E.; Bond, P. J.; Marciniak, S. J.; Kuimova, M. K. An Optical Technique for Mapping Microviscosity Dynamics in Cellular Organelles. *ACS Nano* **2018**, *12*, 4398–4407. (e) López-Duarte, I.; Chairatana, P.; Wu, Y.; Pérez-Moreno, J.; Bennett, P. M.; Reeve, J. E.; Boczarow, I.; Kaluza, W.; Hosny, N. A.; Stranks, S. D.; Nicholas, R. J.; Clays, K.; Kuimova, M. K.; Anderson, H. L. Thiophene-Based Dyes for Probing Membranes. *Org. Biomol. Chem.* **2015**, *13*, 3792–3802. (f) Baumgart, T.; Hunt, G.; Farkas, E. R.; Webb, W. W.; Feigenson, G. W. Fluorescence Probe Partitioning between Lo/Ld Phases in Lipid Membranes.

*Biochim. Biophys. Acta* **2007**, *1768*, 2182–2194. (g) Muraoka, T.; Umetsu, K.; Tabata, K. V.; Hamada, T.; Noji, H.; Yamashita, T.; Kinbara, K. Mechano-Sensitive Synthetic Ion Channels. *J. Am. Chem. Soc.* **2017**, *139*, 18016–18023. (h) Sakai, N.; Houdebert, D.; Matile, S. Voltage-Dependent Formation of Anion Channels by Synthetic Rigid-Rod Push–Pull  $\beta$ -Barrels. *Chem. Eur. J.* **2003**, *9*, 223–232.

(19) Kumpulainen, T.; Rosspeintner, A.; Vauthey, E. Probe Dependence on Polar Solvation Dynamics from Fs Broadband Fluorescence. *Phys. Chem. Chem. Phys.* **2017**, *19*, 8815–8825.

(20) Verolet, Q.; Rosspeintner, A.; Soleimanpour, S.; Sakai, N.; Vauthey, E.; Matile, S. Turn-On Sulfide  $\pi$  Donors: An Ultrafast Push for Twisted Mechanophores. *J. Am. Chem. Soc.* **2015**, *137*, 15644–15647.

(21) Horng, M. L.; Gardecki, J. A.; Papazyan, A.; Maroncelli, M. Subpicosecond Measurements of Polar Solvation Dynamics: Coumarin 153 Revisited. *J. Phys. Chem.* **1995**, *99*, 17311–17337.

(22) (a) Chapman, C. F.; Fee, R. S.; Maroncelli, M. Measurements of the Solute Dependence of Solvation Dynamics in 1-Propanol: The Role of Specific Hydrogen-Bonding Interactions. *J. Phys. Chem.* **1995**, *99*, 4811–4819. (b) Sajadi, M.; Weinberger, M.; Wagenknecht, H.-A.; Ernsting, N. P. Polar Solvation Dynamics in Water and Methanol: Search for Molecularity. *Phys. Chem. Chem. Phys.* **2011**, *13*, 17768–17774.

(23) Periasamy, N.; Teichert, H.; Weise, K.; Vogel, R. F.; Winter, R. Effects of Temperature and Pressure on the Lateral Organization of Model Membranes with Functionally Reconstituted Multidrug Transporter LmrA. *Biochim. Biophys. Acta* **2009**, *1788*, 390–401.

(24) Sharonov, A.; Hochstrasser, R. M. Wide-Field Subdiffraction Imaging by Accumulated Binding of Diffusing Probes. *Proc. Natl. Acad. Sci.* **2006**, *103*, 18911–18916.

(25) Mortensen, K. I.; Churchman, L. S.; Spudich, J. A.; Flyvbjerg, H. Optimized Localization Analysis for Single-Molecule Tracking and Super-Resolution Microscopy. *Nat. Methods* **2010**, *7*, 377–381.

(26) (a) Lew, M. D.; Lee, S. F.; Ptacin, J. L.; Lee, M. K.; Twieg, R. J.; Shapiro, L.; Moerner, W. E. Three-Dimensional Superresolution Colocalization of Intracellular Protein Superstructures and the Cell Surface in Live *Caulobacter Crescentus*. *Proc. Natl. Acad. Sci. USA* **2011**, *108*, E1102–1110. (b) Gomez-

Garcia, P. A.; Garbacik, E. T.; Otterstrom, J. J.; Garcia-Parajo, M. F.; Lakadamyali, M. Excitation-Multiplexed Multicolor Superresolution Imaging with fm-STORM and fm-DNA-PAINT. *Proc. Natl. Acad. Sci. USA* **2018**, *115*, 12991–12996.

